

**REVISITING THE ATTENUATED REFLECTED  
DOWNWARD FLUX TERM OF THE RADIATIVE  
TRANSFER EQUATION**

D.S. Turner

Meteorological Service of Canada

## INTRODUCTION

- assimilation of large amounts of satellite data daily requires fast and accurate radiative transfer models
- LBL's are ill-suited to the task
- a fast parameterized model is an approximation to the LBL
  - approximations are appropriate when compared across a representative of atmospheric state the bias is zero and error is small
  - inappropriate approximations may lead to large bias or systematic errors
- if bias is significant then observations will be used incorrectly by a data assimilation system, resulting in the observations have little impact on the NWPs unless an empirical bias correction scheme is used
  - preferable to avoid, or at least minimize, the use of a bias correction scheme.
  - more effective to minimize, if not eliminate, systematic errors at source
- at MSC, strive to identify sources of systematic error and attempt to eliminate or minimize them
- following study looks at the bias and standard deviation of two models used to approximate the attenuated reflected downward flux term
  - consider NOAA 14 HIRS channels
  - consider AIRS channels, shortlist of 281 channels (M. Goldberg)

The TOA radiance for a plane parallel non-scattering atmosphere (ignoring solar) is the sum of;

- i) attenuated surface emission,
- ii) attenuated upward atmospheric emissions, &
- iii) the attenuated reflected downward flux emissions

$$\mathfrak{R}(\epsilon, \theta, \chi_s) = \int_{\Delta\tilde{v}} \varphi(\tilde{v}) \left[ \epsilon(\tilde{v}) B(\tilde{v}, T(\chi_s)) \mathfrak{S}(\tilde{v}, \theta, \chi_s) + \int_0^{\chi_s} B(\tilde{v}, T(\chi)) \frac{d\mathfrak{S}(\tilde{v}, \theta, \chi)}{d\chi} d\chi \right. + \\ \left. r(\tilde{v}) \mathfrak{S}(\tilde{v}, \theta, \chi_s) \left( 2\pi \int_0^{\chi_s} B(\tilde{v}, T(\chi)) \frac{dE_3(\tilde{v}, \chi' - \chi)}{d\chi} d\chi \right) \right] d\tilde{v} \quad (1)$$

$\epsilon$  - surface emissivity

$r$  - surface reflectivity

$v$  - wavenumber

$\chi$  - optical depth

T - temperature

$\theta$  - satellite zenith

angle

$\mathfrak{S}(\chi)$  - TOA transmittance from  $\chi$

B - Planck function

$E_3$  - 3<sup>rd</sup> exponential  
integral

$\varphi$  - instrument response function

- most parameterized models assume a monochromatic-equivalent model to Eqn 1; eg,  $\langle ab \rangle = \langle a \rangle \langle b \rangle$ .

- simplest approximation to the down flux is to replace it with the downward radiance

for a vertical path in which the optical depths have been scaled

- equivalent to evaluating the radiance along a path defined by the diffusivity angle  $\varphi$ .
- $\sec \varphi$  is known as the diffusivity factor
- downward transmittances written in terms of upward transmittances

- assume emissivity is constant across response function
- reflectivity is isotropic,  $r = (1-\varepsilon)/\pi$

$$\begin{aligned} \mathfrak{R}_\varphi(\varepsilon, \theta, \chi_s) &= \varepsilon \langle B_s \rangle \langle \mathfrak{S}(\theta) \rangle + \sum_{i=0}^s \langle \bar{B}_i \rangle (\langle \mathfrak{S}_{i-1}(\theta) \rangle - \langle \mathfrak{S}_i(\theta) \rangle) + \\ r \langle \mathfrak{S}_s(\theta) \rangle \pi \sum_{i=1}^{s-1} \langle \bar{B}_i \rangle &\frac{\langle \mathfrak{S}_{i-1}(\varphi) \rangle - \langle \mathfrak{S}_i(\varphi) \rangle}{\langle \mathfrak{S}_{i-1}(\varphi) \rangle \langle \mathfrak{S}_i(\varphi) \rangle} \langle \mathfrak{S}_s(\varphi) \rangle \end{aligned} \quad (2)$$

$$\langle \mathbf{f} \rangle = \int \varphi(v) \mathbf{d}v,$$

- Model I, RTTOVS, downward flux approximated by the same path as  $\varphi = \theta$ ,
  - advantage, only one transmittance profile required
  - disadvantage, explicit zenith angle dependency ??
- Model II, constant diffusivity factor,  $\sec \varphi = 1.66$ 
  - disadvantage two transmittance profiles required, slower than model I
  - should be no zenith angle dependency
- ideally, a zero bias accompanied by small error is desirable
  - in practice this is not always obtainable
  - in this study assume any bias below a threshold of .1K is negligible, target value suggested by assimilationists (Chouinard, priv. comm.)

## FAST LINE-BY-LINE SIMULATIONS

- use MSC FLBL radiative transfer model to evaluate  $\mathfrak{R}_{\text{exact}}$  (Eq 1) and all quantities  $\langle \rangle$  in Eq 2
  - evaluating  $\langle \rangle$  directly from the FLBL eliminates any systematic errors due to parameterized models
- use IC2000 atmosphere states
  - 43 levels
  - $\text{H}_2\text{O}$ ,  $\text{CO}_2$ ,  $\text{O}_3$ ,  $\text{N}_2\text{O}$ ,  $\text{CO}$ ,  $\text{CH}_4$ ,  $\text{CO}_2$ ,  $\text{O}_2$  &  $\text{N}_2$
- for each of the 42 IC2000 atmospheric states simulations are done for
  - 6 values of emissivity,  $\epsilon = 1, .98, .96, .94, .92, .\& 9$
  - 5 satellite zenith angles,  $\sec \theta = 1, 1.25, 1.5, 1.75, \& 2$
  - 8 surface pressures,  $p_{\text{surf}} 168.95, 253.71, 396.81, 521.46, 749.12 \& 1013.25 \text{ mb}$ 
    - wide range of surface pressures accounts for a wide range of topographical surfaces and cloud top pressures
- consider NOAA 14 HIRS channels and 279 (of 2378) AIRS channels (Golberg)
- Planck-weighted transmittances are used where appropriate (Turner 2000)
- bias and standard deviations of  $\Delta T$  evaluated for all combinations of  $\epsilon, \theta$  &  $p_{\text{surf}}$  for each model

$$\Delta T(\epsilon, \theta, p_s) = BT(\mathfrak{R}(\epsilon, \theta, p_s)) - BT(\mathfrak{R}_\phi(\epsilon, \theta, p_s)) \quad (5)$$

NOTE: Many of the following graphs are plotted against channel index. A table of channel index vs wavenumber is located on the last 2 pages.

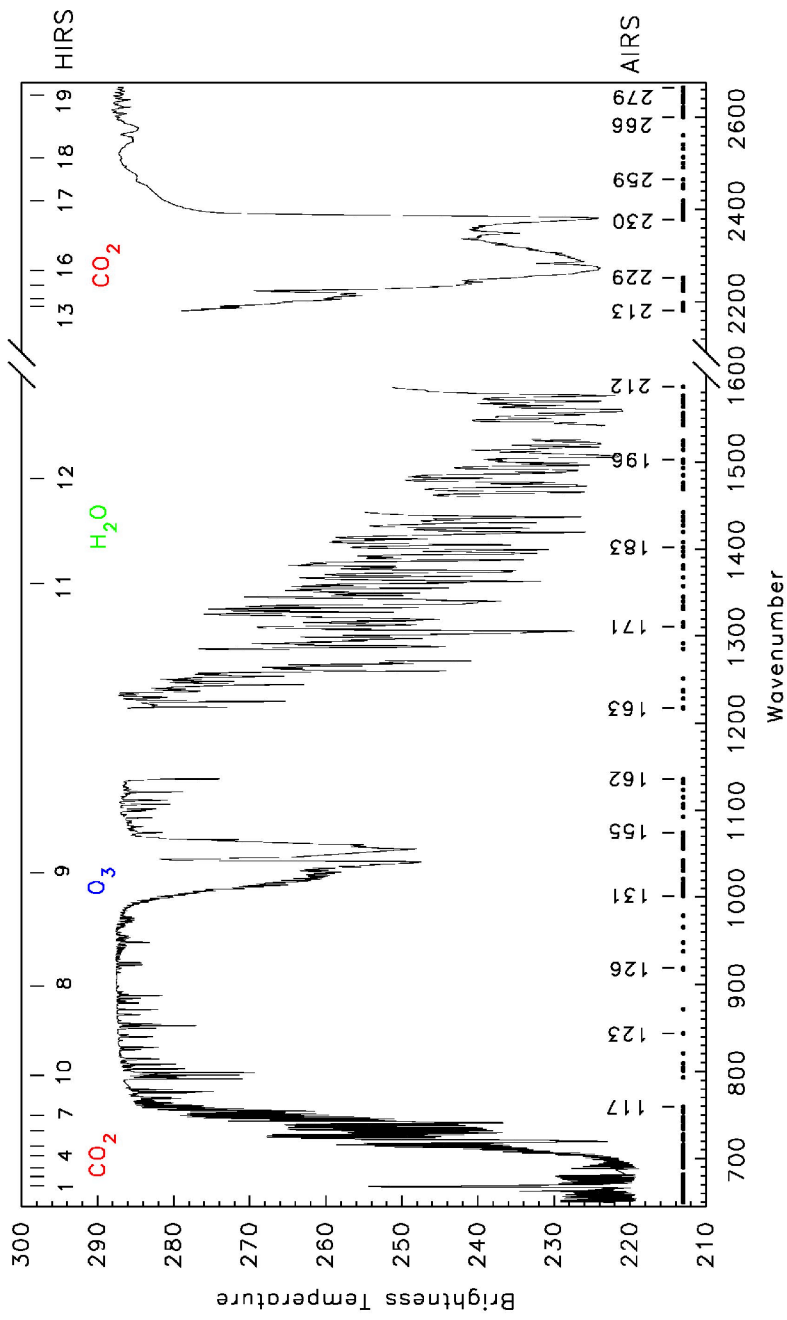


Fig 1: BT spectra for the US standard atmosphere for a surface pressure of 1013.25mb and  $\epsilon=1$ . The central positions of the NOAA 14 HIRS channels are indicated at the top and the positions of the AIRS channels listed in column A of table I are indicated along the bottom.

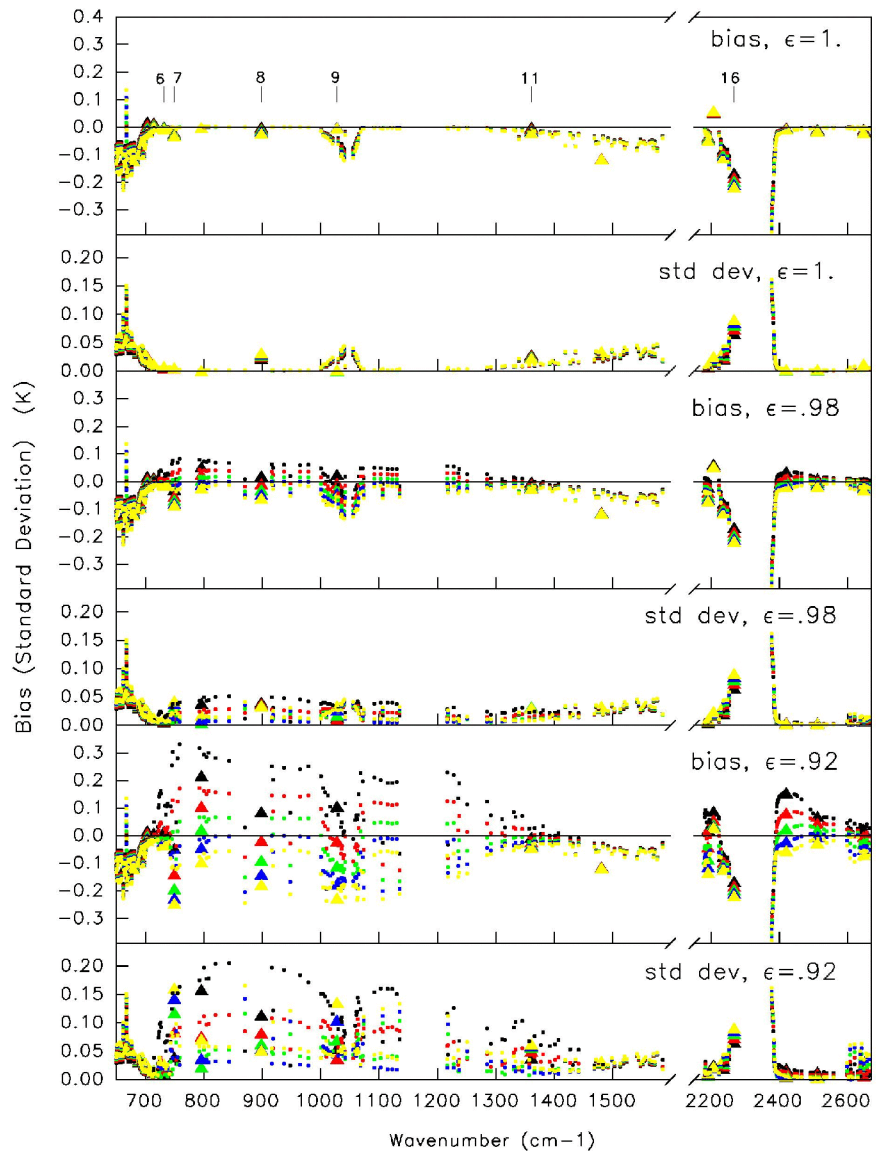


Fig 1: Plot of Model I bias and standard deviation of  $\Delta BT$  over 42 profiles for HIRS  $\blacktriangle$  and AIRS  $\cdot$  assuming a surface pressure of 1013.25mb for 5 zenith angles;  $\blacktriangle$   $\sec\theta=1$ ,  $\blacktriangle$   $\sec\theta=1.25$ ,  $\blacktriangle$   $\sec\theta=1.5$ ,  $\blacktriangle$   $\sec\theta=1.75$  and  $\blacktriangle$   $\sec\theta=2$ . The labelled "||" in the uppermost box marks the spectral locations of the HIRS channels specified in Fig 2.

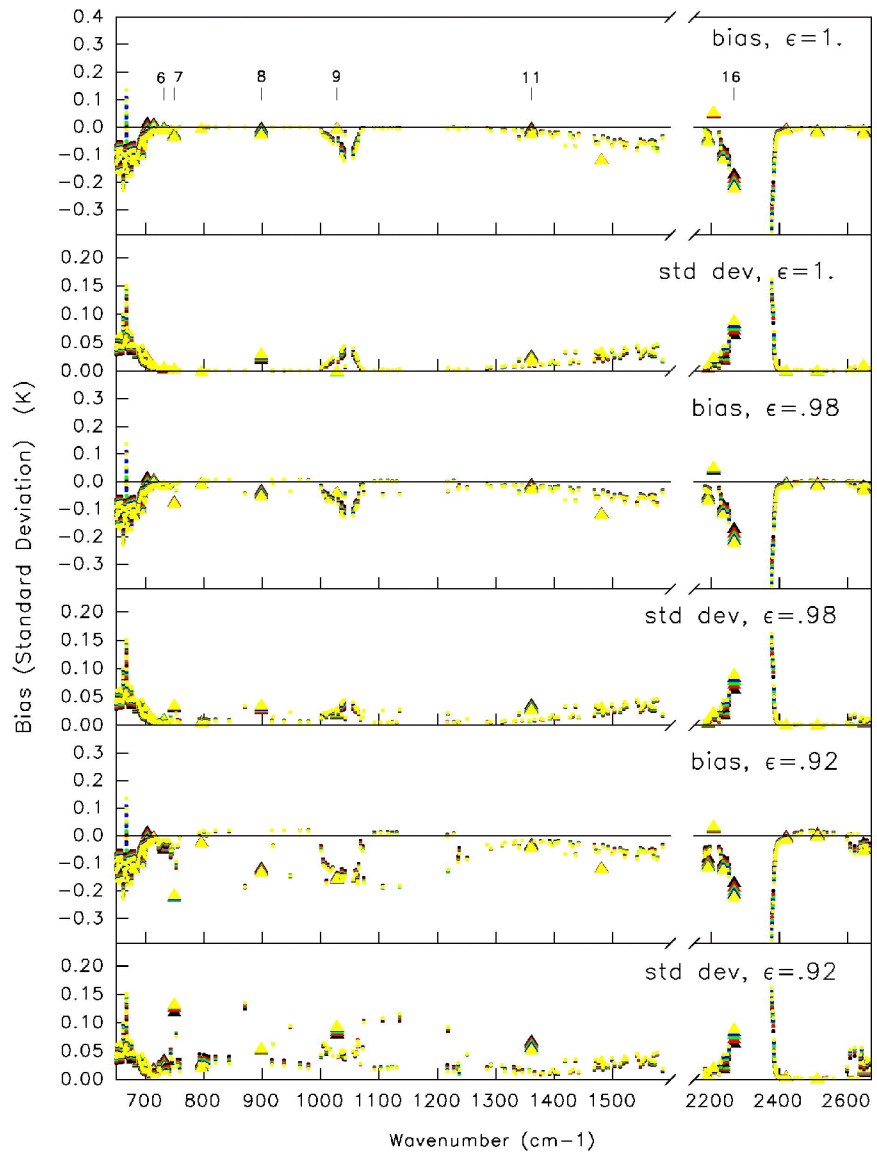
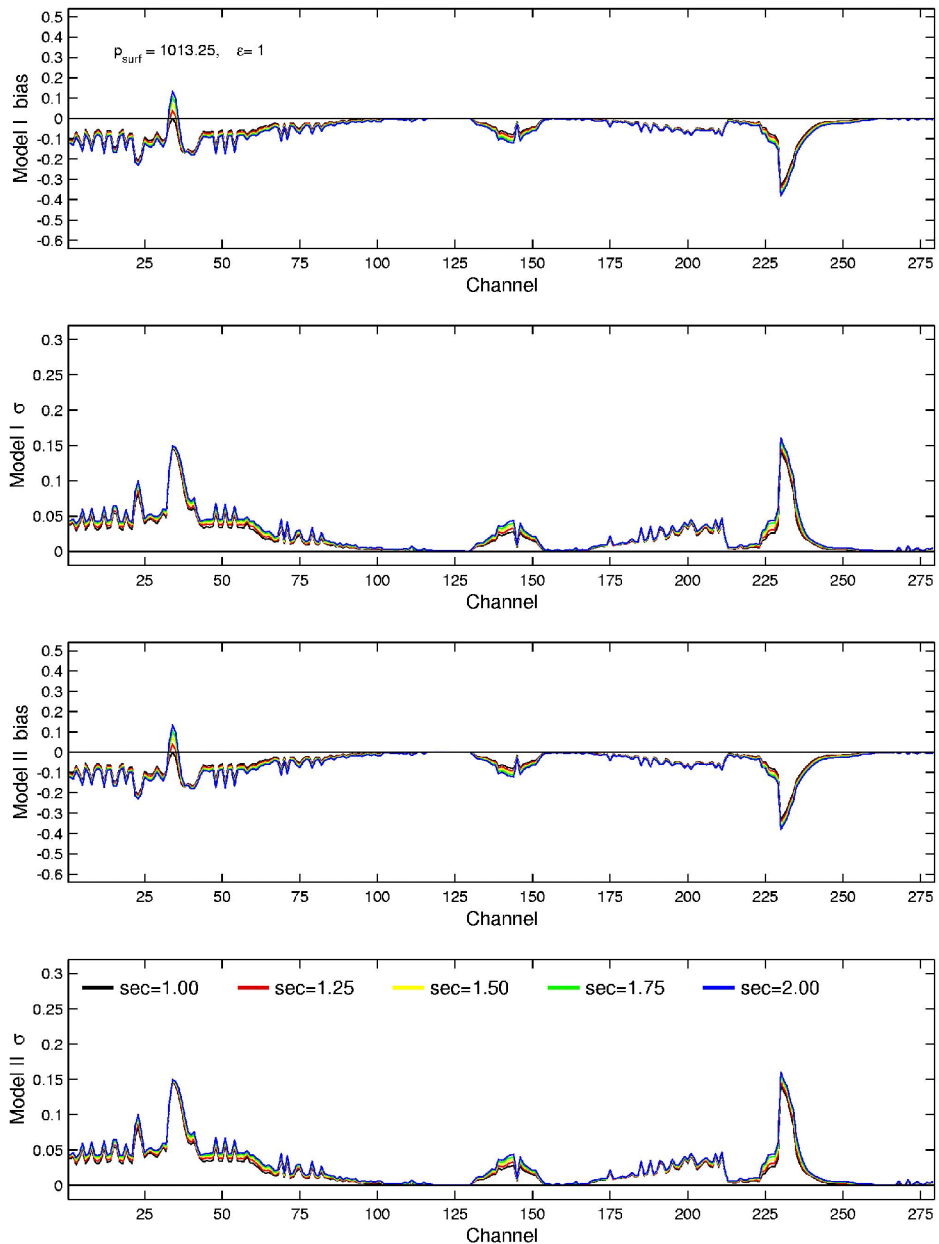
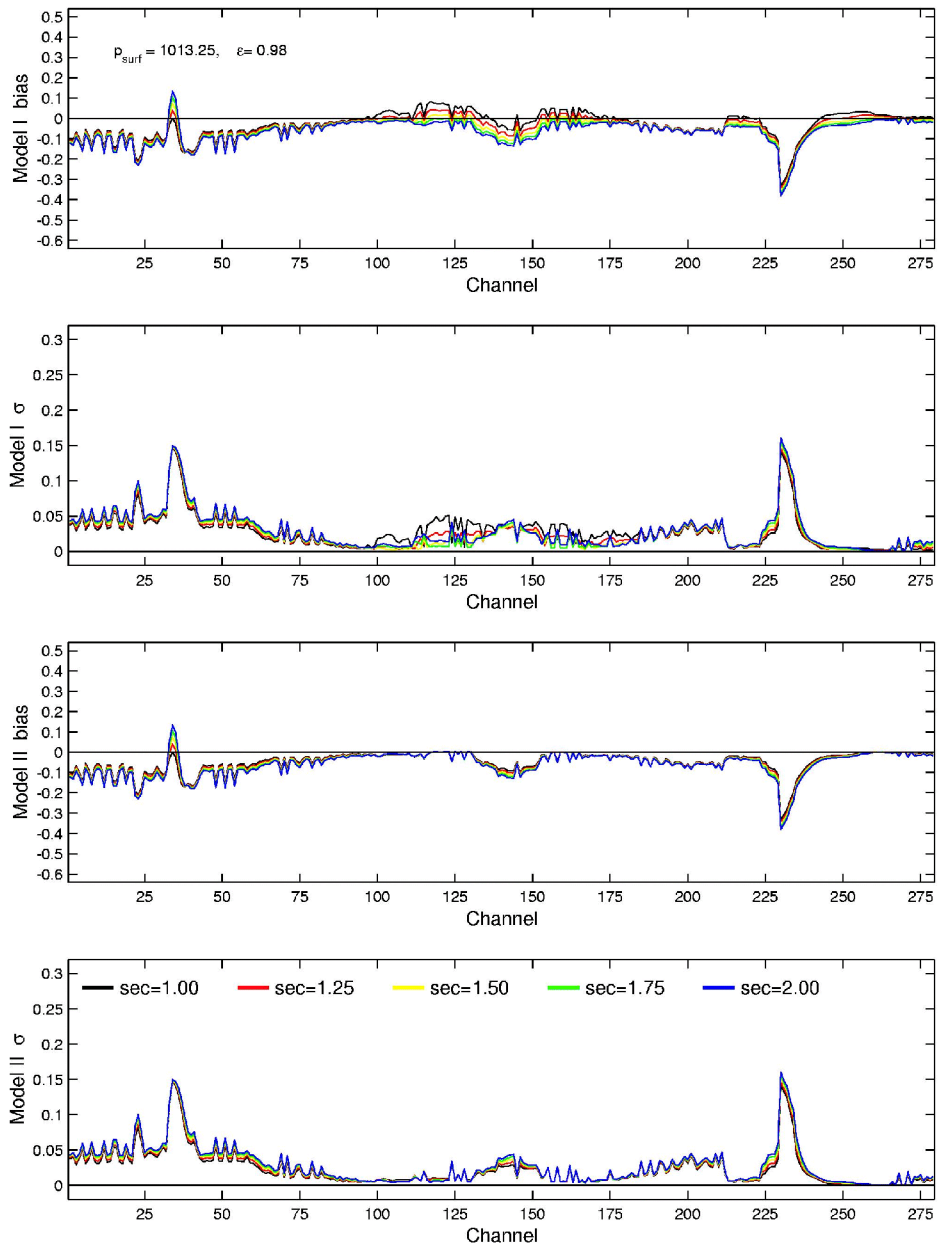


Fig 3: Plot of Model II bias and standard deviation of  $\Delta BT$  over 42 profiles for HIRS  $\blacktriangle$  and AIRS  $\cdot$  assuming a surface pressure of 1013.25mb for 5 zenith angles;  $\blacktriangle$   $\sec\theta=1$ ,  $\blacktriangle$   $\sec\theta=1.25$ ,  $\blacktriangle$   $\sec\theta=1.5$ ,  $\blacktriangle$   $\sec\theta=1.75$  and  $\blacktriangle$   $\sec\theta=2$ . The labeled "||" in the uppermost box marks the spectral locations of the HIRS channels specified in Fig 4.



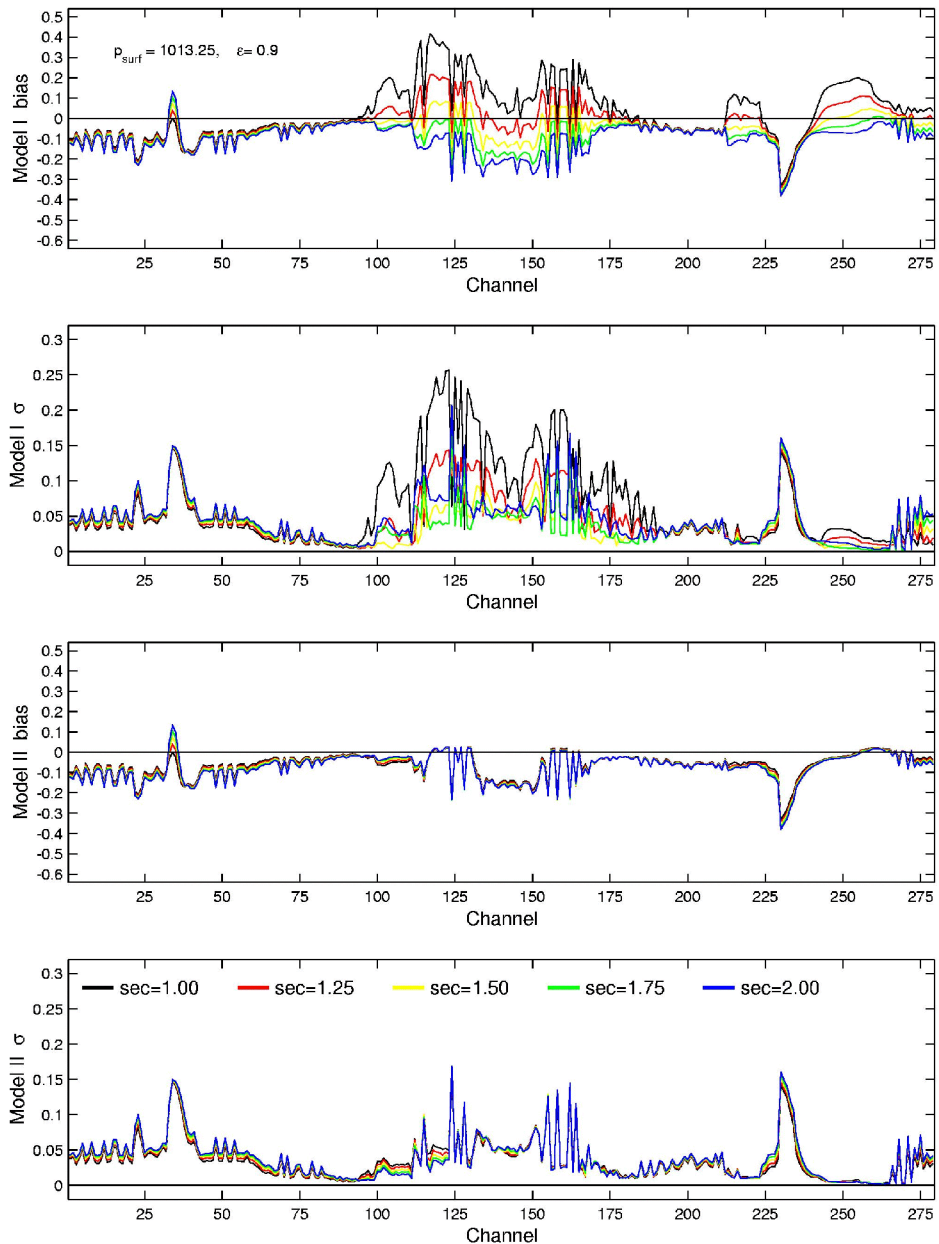
Fig##: Bias and standard deviation of the AIRS BT difference between the FLBL and models I and II over 42 profiles. The surface pressure is 1013.25mb and  $\epsilon$  is 1. The calculation is done for 5 zenith angles;

06-Feb-2002 09:57:56 a\_61p6.p2



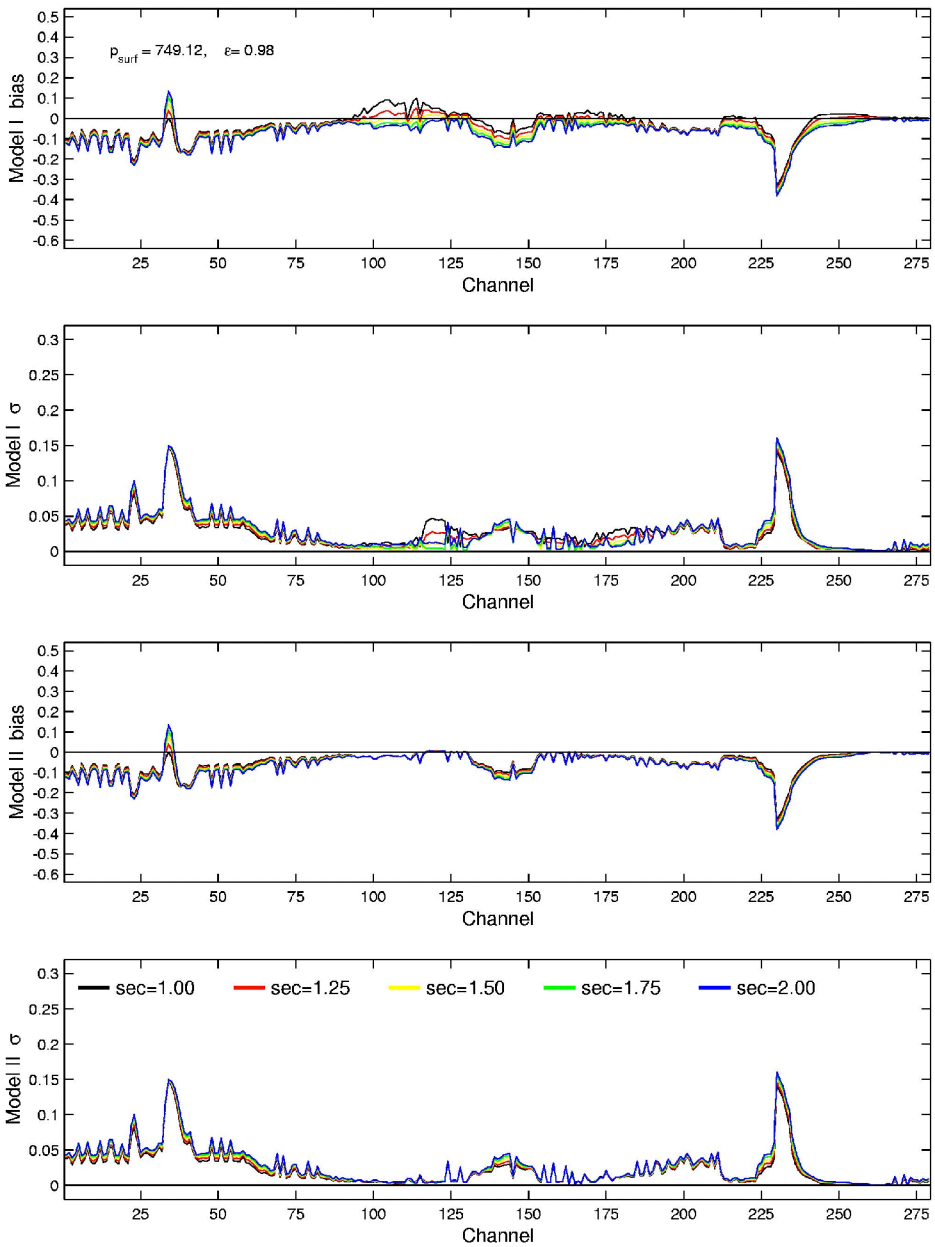
Fig##: Bias and standard deviation of the AIRS BT difference between the FLBL and models I and II over 42 profiles. The surface pressure is 1013.25mb and  $\varepsilon$  is 0.98. The calculation is done for 5 zenith angles;

06-Feb-2002 09:58:00 a\_e2p6.p2



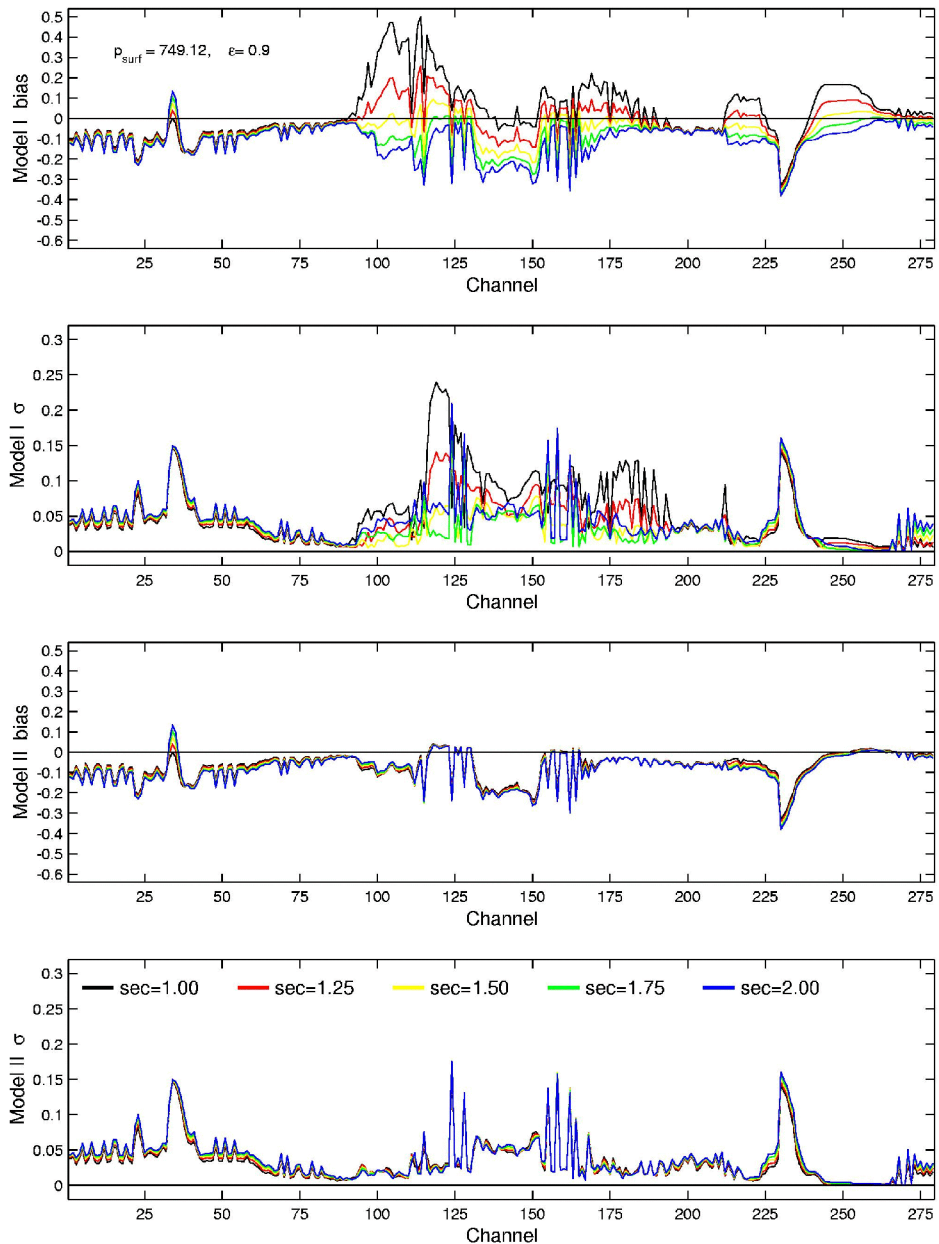
Fig##: Bias and standard deviation of the AIRS BT difference between the FLBL and models I and II over 42 profiles. The surface pressure is 1013.25mb and  $\epsilon$  is 0.9. The calculation is done for 5 zenith angles;

06-Feb-2002 09:58:13 a\_6ep6.p2



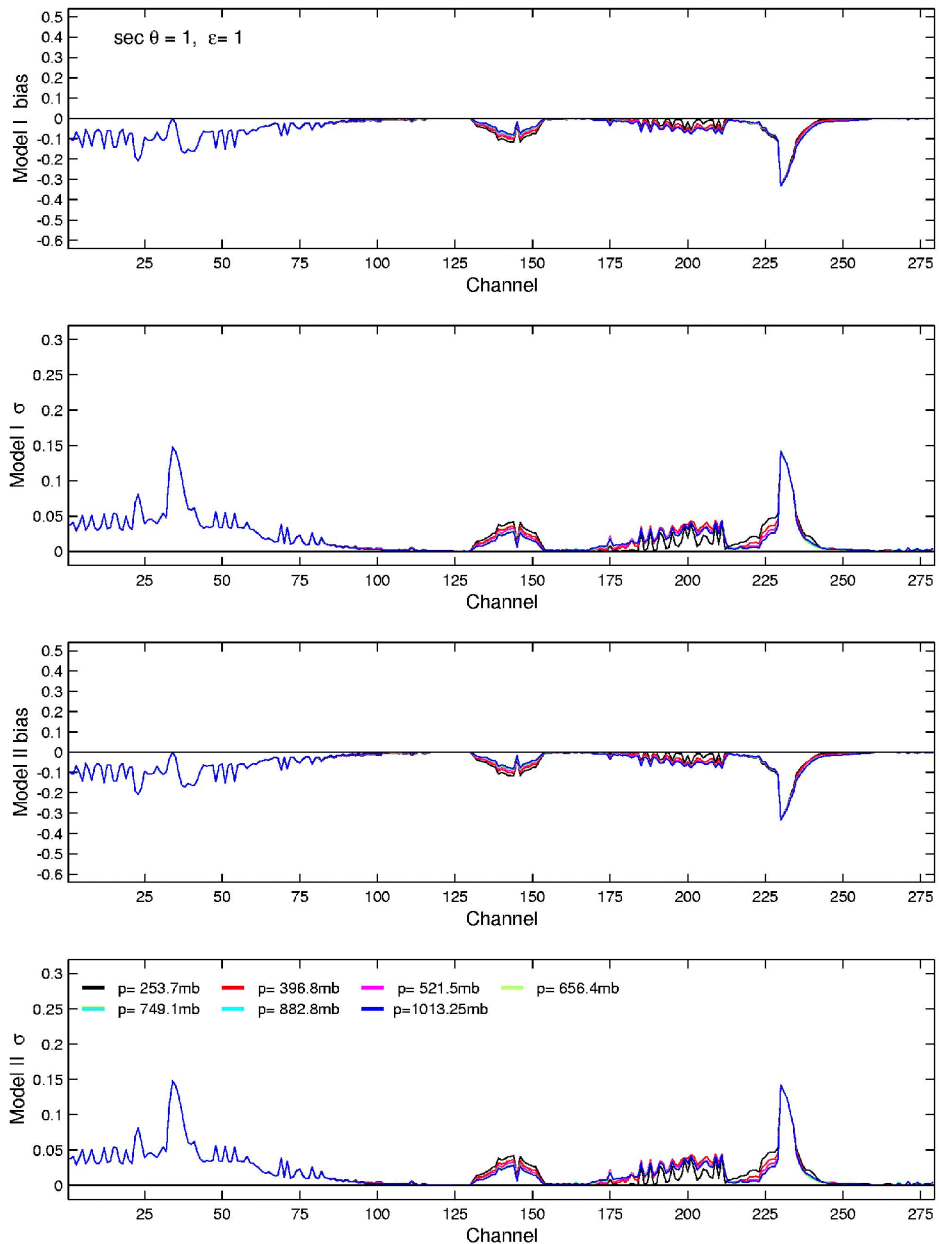
Fig##: Bias and standard deviation of the AIRS BT difference between the FLBL and models I and II over 42 profiles. The surface pressure is 749.12mb and  $e$  is 0.98. The calculation is done for 5 zenith angles;

06-Feb-2002 09:57:59 a\_82p6.p2



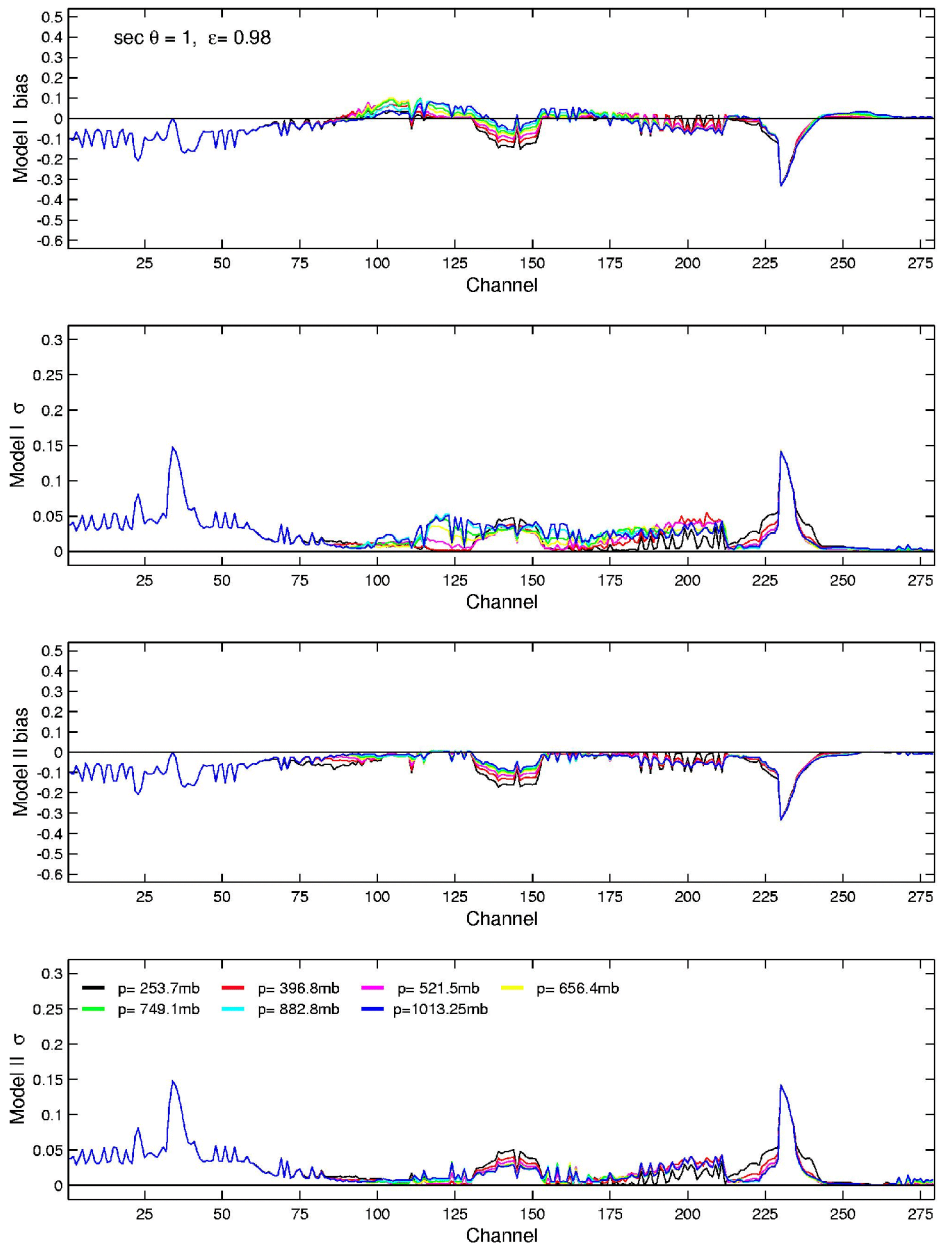
Fig##: Bias and standard deviation of the AIRS BT difference between the FLBL and models I and II over 42 profiles. The surface pressure is 749.12mb and  $e$  is 0.9. The calculation is done for 5 zenith angles;

06-Feb-2002 09:58:12 a\_6fp6.p2



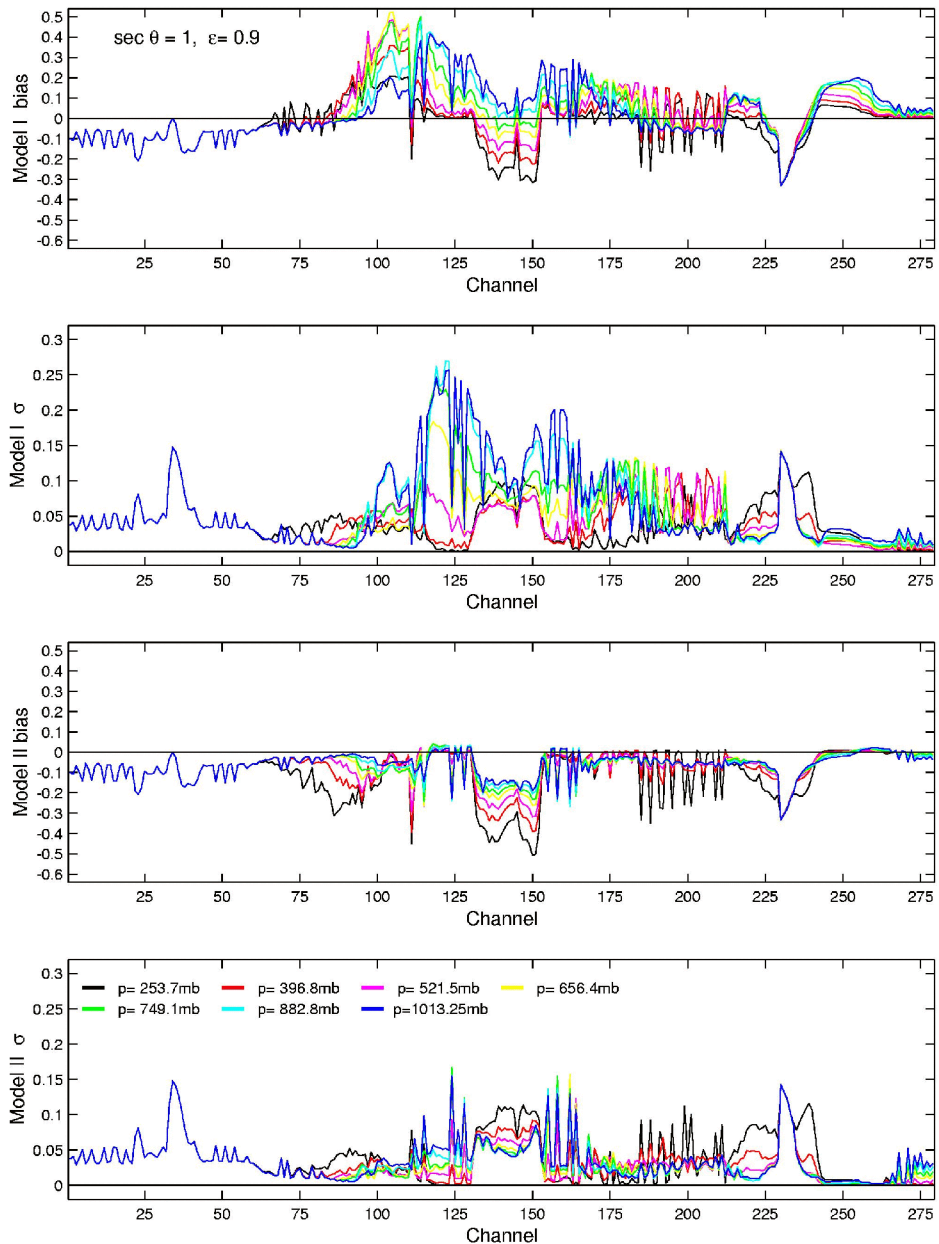
Fig##: Bias and standard deviation of the AIRS BT difference between the FLBL and models I and II over 42 profiles. The zenith angle secant is 1 and  $\varepsilon = 1$ . The calculation is done for 7 surface pressures.

06-Feb-2002 11:16:45 a\_e121.124



Fig##: Bias and standard deviation of the AIRS BT difference between the FLBL and models I and II over 42 profiles. The zenith angle secant is 1 and  $\varepsilon = 0.98$ . The calculation is done for 7 surface pressures.

06-Feb-2002 11:18:54 a\_621.3d



Fig##: Bias and standard deviation of the AIRS BT difference between the FLBL and models I and II over 42 profiles. The zenith angle secant is 1 and  $\varepsilon = 0.9$ . The calculation is done for 7 surface pressures.

06-Feb-2002 11:19:51 a\_06x1.3d

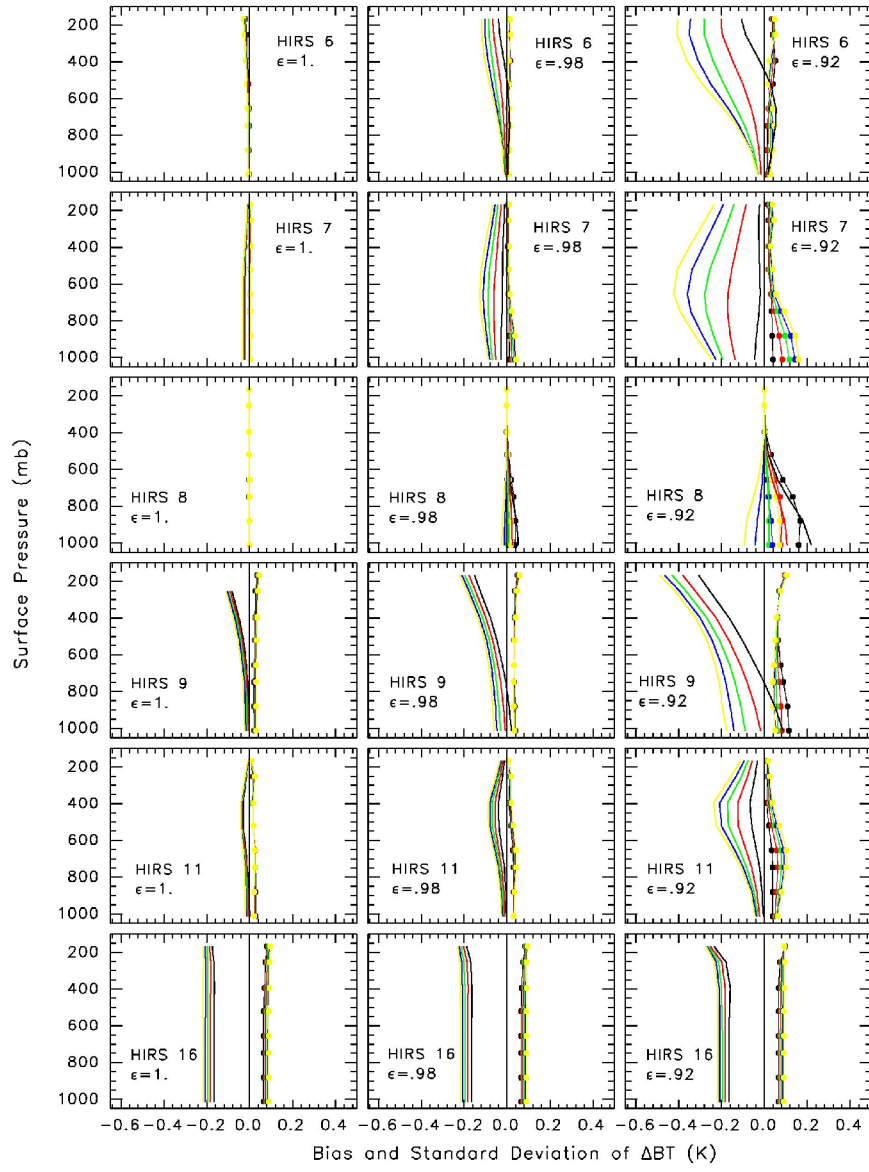


Fig. 2 Bias — and standard deviation • of  $\Delta BT$  over 42 profiles for Model I. The comparison is done as a function of surface pressure, emissivity, and satellite zenith angle; —  $\sec\theta=1$ , —  $\sec\theta=1.25$ , —  $\sec\theta=1.5$ , —  $\sec\theta=1.75$  and —  $\sec\theta=2$ . HIRS 6 and 16 were evaluated using Planck-weighted transmittances.

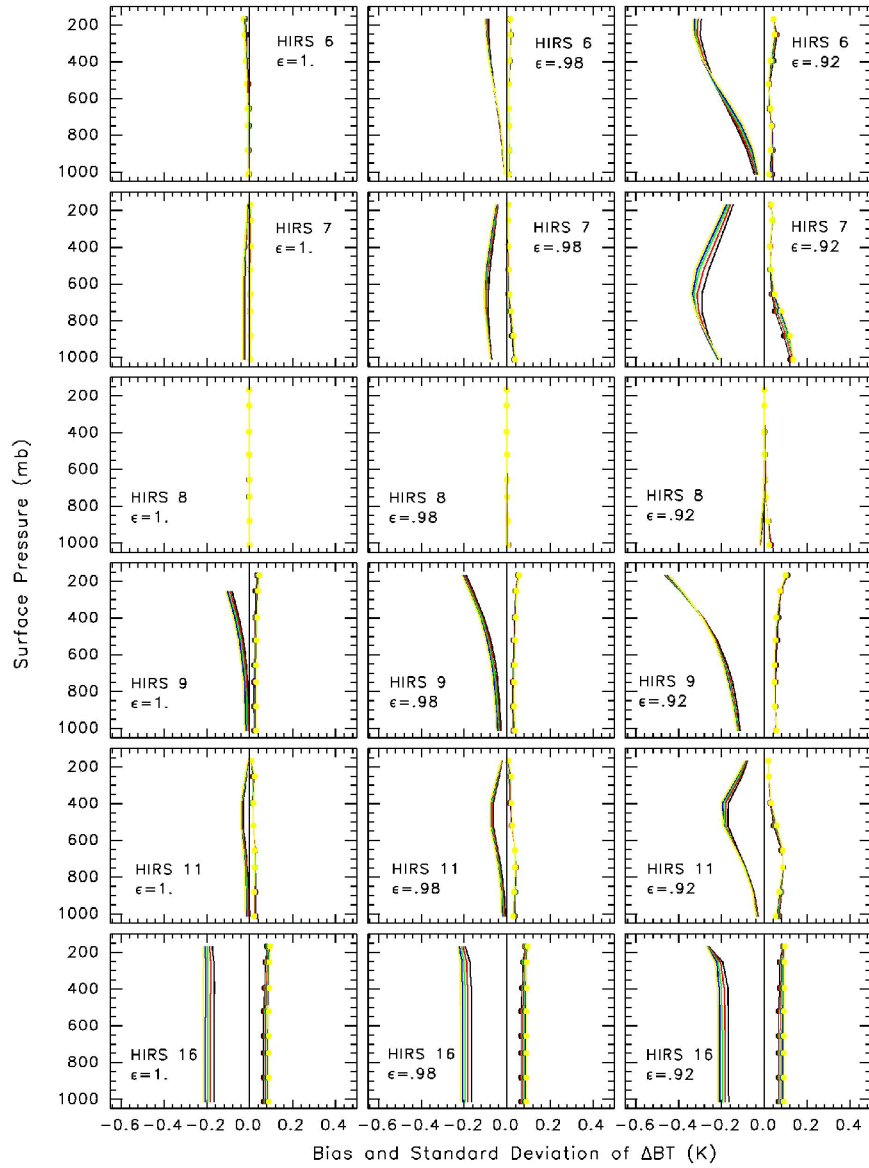


Fig. 4 Bias — and standard deviation • of  $\Delta BT$  over 42 profiles for Model II. The comparison is done as a function of surface pressure, emissivity, and satellite zenith angle; —  $\sec\theta=1$ , —  $\sec\theta=1.25$ , —  $\sec\theta=1.5$ , —  $\sec\theta=1.75$  and —  $\sec\theta=2$ . HIRS 6 and 16 were evaluated using Planck-weighted transmittances.

## SUMMARY

- RTTOVS has systematic errors that are zenith angle dependent and surface pressure dependent
  - bias range from < .1K upto .5K
  - current approximation is acceptable for most clear sky circumstances
    - $\epsilon > .97$
    - $p_{\text{surf}} > 800\text{mb}$
  - surface pressure dependency has vertical structure
  - potential problems
    - for a small range of surface cases
    - cloudy radiances
      - eg potential problem for detection of cloud tops if  $\epsilon < .98$
- Model II has surface pressure (cloud top) dependency
  - eliminates satellite zenith angle dependency
  - has potential problems for cloudy radiances
  - gain is small, questionable as to whether algorithm is worth the extra computational expense

## FUTURE WORK

- pressure dependency is likely due to assuming a constant diffusivity factor for all layers
  - diffusivity factor depends on vertical optical depth above  $p_{\text{surf}}$
  - diffusivity factor can vary from 1 to 2 for a homogenous layer
- attempt to modify the downward transmittance profile in model II with a pressure dependent parameter to one more suitable
  - still requires two transmittance profiles to be evaluated
- may be possible to modify RTTOVS transmittance profile to a suitable downward transmittance profile with extra parameters
  - small increase in computational expense, if not too complicated
  - in addition may provide a starting point for a similar parameterization for handling solar transmission term

<b>A</b>	<b>B</b>	v	<b>A</b>	<b>B</b>	v	<b>A</b>	<b>B</b>	v	<b>A</b>	<b>B</b>	v	<b>A</b>	<b>B</b>	v
1	1	649.548	57	123	680.071	113	333	745.928	169	1371	1285.323	225	1918	2230.281
2	6	650.742	58	124	680.333	114	338	747.517	170	1382	1291.555	226	1924	2235.968
3	7	650.981	59	128	681.386	115	355	752.970	171	1415	1310.607	227	1928	2239.775
4	10	651.700	60	129	681.650	116	362	755.237	172	1424	1315.898	228	1937	2248.388
5	11	651.940	61	138	689.418	117	375	759.485	173	1449	1330.813	229	1941	2252.236
6	15	652.903	62	139	689.689	118	453	793.074	174	1455	1334.442	230	2099	2378.164
7	16	653.144	63	144	691.046	119	475	801.001	175	1466	1339.549	231	2100	2379.133
8	17	653.385	64	145	691.318	120	484	804.287	176	1477	1345.174	232	2101	2380.103
9	20	654.110	65	150	692.681	121	497	809.080	177	1500	1357.094	233	2103	2382.045
10	21	654.351	66	151	692.955	122	528	820.731	178	1519	1367.110	234	2104	2383.017
11	22	654.594	67	156	694.325	123	587	843.805	179	1538	1377.280	235	2106	2384.964
12	24	655.079	68	157	694.600	124	672	871.201	180	1545	1381.066	236	2107	2385.938
13	27	655.807	69	159	695.150	125	787	917.209	181	1565	1392.004	237	2108	2386.914
14	28	656.051	70	162	695.977	126	791	918.649	182	1574	1396.985	238	2109	2387.890
15	30	656.538	71	165	696.806	127	843	937.807	183	1583	1402.002	239	2110	2388.867
16	36	658.004	72	168	697.637	128	870	948.080	184	1593	1407.620	240	2111	2389.845
17	39	658.740	73	169	697.915	129	914	965.323	185	1614	1419.570	241	2112	2390.824
18	40	658.985	74	170	698.192	130	950	979.017	186	1627	1427.072	242	2113	2391.803
19	42	659.477	75	172	698.748	131	1003	1001.268	187	1636	1432.313	243	2114	2392.784
20	51	661.700	76	173	699.027	132	1012	1005.146	188	1644	1437.005	244	2115	2393.765
21	52	661.948	77	174	699.305	133	1019	1008.182	189	1652	1441.728	245	2116	2394.747
22	54	662.445	78	175	699.584	134	1024	1010.362	190	1669	1468.661	246	2117	2395.729
23	55	662.693	79	177	700.142	135	1030	1012.991	191	1674	1471.743	247	2118	2396.713
24	56	662.942	80	179	700.702	136	1038	1016.516	192	1681	1476.079	248	2119	2397.697
25	59	663.690	81	180	700.982	137	1048	1020.956	193	1694	1484.199	249	2120	2398.683
26	62	664.439	82	182	701.542	138	1069	1030.405	194	1708	1493.043	250	2121	2399.669
27	63	664.689	83	185	702.385	139	1079	1034.965	195	1717	1498.784	251	2122	2400.656
28	68	665.943	84	186	702.666	140	1082	1036.341	196	1723	1502.636	252	2123	2401.643
29	69	666.194	85	190	703.794	141	1083	1036.800	197	1740	1513.655	253	2128	2406.594
30	71	666.698	86	192	704.359	142	1088	1039.102	198	1748	1518.896	254	2134	2412.563
31	72	666.950	87	198	706.060	143	1090	1040.026	199	1751	1520.871	255	2141	2419.564
32	73	667.202	88	201	706.914	144	1092	1040.951	200	1756	1524.173	256	2145	2445.918
33	74	667.454	89	204	707.770	145	1095	1042.343	201	1763	1542.266	257	2149	2450.020
34	75	667.707	90	207	708.628	146	1104	1055.975	202	1766	1544.299	258	2153	2454.135
35	76	667.959	91	210	709.488	147	1111	1059.314	203	1771	1547.697	259	2164	2465.523
36	77	668.212	92	215	710.927	148	1115	1061.231	204	1777	1551.795	260	2189	2491.792
37	78	668.465	93	216	711.215	149	1116	1061.711	205	1780	1553.852	261	2197	2500.313
38	79	668.719	94	221	712.661	150	1119	1063.155	206	1783	1555.915	262	2209	2513.202

<b>A</b>	<b>B</b>	<b>v</b>												
39	80	668.972	95	226	714.112	151	1120	1063.637	207	1794	1563.522	263	2226	2531.682
40	82	669.480	96	227	714.403	152	1123	1065.085	208	1800	1567.701	264	2234	2540.470
41	83	669.734	97	232	715.862	153	1130	1068.479	209	1803	1569.799	265	2280	2560.853
42	84	669.989	98	252	721.758	154	1138	1072.383	210	1806	1571.903	266	2318	2600.214
43	86	670.498	99	253	722.055	155	1142	1074.345	211	1812	1576.126	267	2321	2603.375
44	92	672.031	100	256	722.949	156	1178	1092.314	212	1826	1586.065	268	2325	2607.601
45	93	672.287	101	257	723.247	157	1199	1103.060	213	1865	2181.250	269	2328	2610.779
46	98	673.572	102	261	724.443	158	1206	1106.686	214	1866	2182.155	270	2333	2616.095
47	99	673.829	103	262	724.742	159	1221	1114.532	215	1868	2183.968	271	2339	2622.503
48	101	674.345	104	267	726.244	160	1237	1123.017	216	1869	2184.876	272	2348	2632.175
49	104	675.119	105	272	727.752	161	1252	1131.082	217	1872	2187.604	273	2353	2637.580
50	105	675.378	106	295	734.067	162	1260	1135.428	218	1873	2188.515	274	2355	2639.748
51	108	676.156	107	299	735.298	163	1263	1216.837	219	1876	2191.251	275	2357	2641.920
52	110	676.675	108	300	735.607	164	1266	1218.359	220	1881	2195.827	276	2363	2648.457
53	111	676.935	109	305	737.152	165	1285	1228.086	221	1882	2196.745	277	2370	2656.126
54	113	677.455	110	310	738.704	166	1301	1236.397	222	1883	2197.663	278	2371	2657.225
55	116	678.238	111	321	742.142	167	1304	1237.968	223	1911	2223.682	279	2377	2663.839
56	117	678.499	112	325	743.400	168	1329	1251.212	224	1917	2229.336			

Table of the channel indices used in the figures, column A, cross-referenced to the AIRS channel index, column B, and, v, the response functions reference wavenumber (cm.-1)